Published December 6, 2016

Estrogen activation of microglia underlies the sexually dimorphic differences in *Nf1* optic glioma–induced retinal pathology

Joseph A. Toonen, Anne C. Solga, Yu Ma, and David H. Gutmann

Department of Neurology, Washington University School of Medicine, St. Louis, MO 63110

Children with neurofibromatosis type 1 (NF1) develop low-grade brain tumors throughout the optic pathway. Nearly 50% of children with optic pathway gliomas (OPGs) experience visual impairment, and few regain their vision after chemotherapy. Recent studies have revealed that girls with optic nerve gliomas are five times more likely to lose vision and require treatment than boys. To determine the mechanism underlying this sexually dimorphic difference in clinical outcome, we leveraged *Nf1* optic glioma (*Nf1*-OPG) mice. We demonstrate that female *Nf1*-OPG mice exhibit greater retinal ganglion cell (RGC) loss and only females have retinal nerve fiber layer (RNFL) thinning, despite mice of both sexes harboring tumors of identical volumes and proliferation. Female gonadal sex hormones are responsible for this sexual dimorphism, as ovariectomy, but not castration, of *Nf1*-OPG mice normalizes RGC survival and RNFL thickness. In addition, female *Nf1*-OPG mice have threefold more microglia than their male counterparts, and minocycline inhibition of microglia corrects the retinal pathology. Moreover, pharmacologic inhibition of microglial estrogen receptor-β (ERβ) function corrects the retinal abnormalities in female *Nf1*-OPG mice. Collectively, these studies establish that female gonadal sex hormones underlie the sexual dimorphic differences in *Nf1* optic glioma–induced retinal dysfunction by operating at the level of tumor-associated microglial activation.

INTRODUCTION

Neurofibromatosis type 1 (NF1) is a monogenic cancer predisposition syndrome that results from germline mutations in the *NF1* tumor suppressor gene and predisposes affected individuals to develop benign and malignant tumors. One of the significant clinical challenges in managing children and adults with NF1 is the extreme clinical heterogeneity of the disease. In this regard, 15–20% of children with NF1 develop low-grade astrocytomas along the optic pathway, termed optic pathway gliomas (OPGs; Listernick et al., 1994). These tumors, characterized by low proliferative indices and infiltration of microglia, lead to visual impairment in 30–50% of children with NF1-OPGs. Unfortunately, this decline in visual acuity is frequently irreversible after successful chemotherapy (Kalin-Hajdu et al., 2014). In addition, it is not clear which child with an NF1-OPG will experience visual decline and require treatment, necessitating that all young children with NF1 undergo annual ophthalmological evaluations to identify those with reduced visual acuity using age-appropriate visual tests (Listernick et al., 2007). Moreover, these assessments require that preverbal children cooperate and fully engage during the examination, which is often challenging for children with NF1 who harbor comorbid attention deficits (Hyman et al., 2005).

To identify potential risk factors for OPG-induced visual decline, we recently found that girls with NF1 are more likely to lose vision and require treatment than boys (Diggs-Andrews et al., 2014b). Importantly, when segmented by tumor location within the optic pathway, girls with optic nerve gliomas were 5–10 times more likely to experience visual decline than their male counterparts (Diggs-Andrews et al., 2014a; Fisher et al., 2014). Because boys and girls with NF1 develop OPGs at relatively similar frequencies, these findings indicate that a sexually dimorphic effect may underlie OPG-induced vision loss.

In this study, we leveraged an *Nf1* genetically engineered mouse strain that similarly exhibits sexually dimorphic differences in optic glioma–induced visual acuity impairment to define the molecular and cellular basis for these effects (Diggs-Andrews et al., 2014b). We demonstrate, for the first time, that female gonadal sex hormones are responsible for increased retinal ganglion cell (RGC) loss and retinal nerve fiber layer (RNFL) thinning secondary to murine optic glioma, which reflects estrogen receptor activation of tumor-associated microglia. Together, these findings establish that

Correspondence to David H. Gutmann: gutmannd@wustl.edu

Abbreviations used: FF, $Nf1^{flox/flox}$; IPL-GCL, inner plexiform layer-ganglion cell layer; NF1, neurofibromatosis type 1; OPG, optic pathway glioma; OVX, ovariectomized; PHTPP, 4-[2-phenyl-5,7-bis(trifluoromethyl)pyrazolo[1,5-a]-pyrimidin-3-yl]phenol; pNF-H, phospho-neurofilament heavy chain; RGC, retinal ganglion cell; RNFL, retinal nerve fiber layer; VCD, 4-vinylcyclohexene diepoxide.

The Rockefeller University Press $30.00
J. Exp. Med. 2017 Vol. 214 No. 1 17–25
https://doi.org/10.1084/jem.20160447

Published December 6, 2016

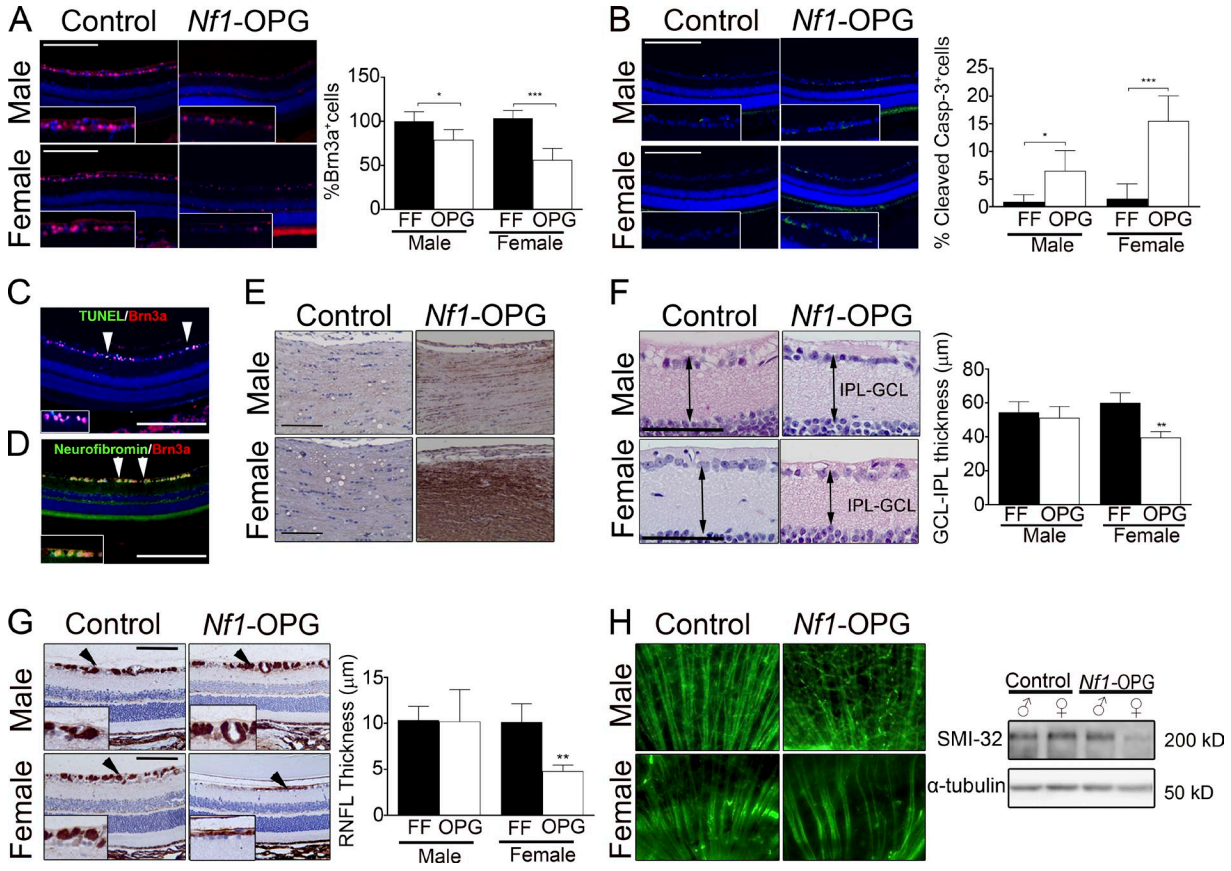

Figure 1. **Retinal dysfunction is sexually dimorphic in *Nf1*-OPG mice.** (A) The percentage of Brn3a$^+$ RGCs was decreased in female *Nf1*-OPG mice (mean, 56.13 ± 13.11% SD; n = 7 mice) compared with FF controls (103.6 ± 8.6%; n = 7 mice), and to a lesser degree in their male counterparts (FF males, 100 ± 10.91%; n = 7 mice; *Nf1*-OPG males, 79.01 ± 11.6%; n = 7 mice). (B) Cleaved caspase-3$^+$ cells were increased in female *Nf1*-OPG mice (15.52 ± 4.52%; n = 6 mice) compared with FF controls (1.45 ± 1.09%; n = 6 mice), but were less elevated in male *Nf1*-OPG mice (0.822 ± 1.29%; n = 8 mice) relative to FF controls (6.451 ± 3.72%; n = 6 mice). (C) Double-labeled Brn3a$^+$ (red) and TUNEL$^+$ cells (green) were detected in female *Nf1*-OPG mice. (D) Neurofibromin (green) was primarily expressed in Brn3a$^+$ (red) RGCs in WT mice. (E) pNF-H immunostaining was detected in the optic nerves of female *Nf1*-OPG mice, but not *Nf1*-OPG males or controls. (F) IPL-GCL layer thickness showed no differences in males (FF, 54.41 ± 6.3 µm; n = 6 mice; OPG, 51.23 ± 6.67 µm; n = 6 mice), whereas thinning was found in *Nf1*-OPG females (39.54 ± 3.55 µm; n = 7 mice) compared with controls (FF, 60.1 ± 5.96 µm; n = 6 mice). (G) SMI-32 staining (RNFL thickness) revealed thinning in female *Nf1*-OPG retinae (4.82 ± 0.64 µm; n = 6 mice) relative to controls (10.14 ± 1.99 µm; n = 6 mice). No differences were seen in males (FF, 10.37 ± 1.5 µm; n = 6 mice; OPG, 10.22 ± 3.46 µm; n = 6 mice). (H) Decreased SMI-32 staining was observed in female *Nf1*-OPG retinal flatmounts (left) and by immunoblotting (right). Data in A, B, F, and G were analyzed using a one-way ANOVA (Kruskal-Wallis test) with a Dunn's multiple comparison post-test. Similar results were obtained in a second independent experiment containing six mice per group. Bars, 100 µm. *, $P < 0.05$; **, $P < 0.01$; ***, $P < 0.001$.

female gonadal sex hormones act as microglial activators in the pathogenesis of NF1-OPG visual decline.

RESULTS AND DISCUSSION

RGC death and RNFL loss are sexually dimorphic in *Nf1*-OPG mice

To define the molecular and cellular basis underlying the observed sexually dimorphic visual decline in children with NF1-OPG, we used a credentialed *Nf1*-OPG genetically engineered mouse strain (Bajenaru et al., 2003), in which optic nerve and chiasmal gliomas form by 3 mo of age, and mice exhibit decreased visual acuity in a sexually dimorphic manner by 6 mo of age (Diggs-Andrews et al., 2014b). A 56% reduction in RGC numbers (% Brn3a$^+$ cells) was observed in female *Nf1*-OPG mice relative to controls (*Nf1*$^{flox/flox}$ mice [FF]), with only minor changes in their male counterparts (Fig. 1 A). The reduction in RGC number was caused by increased apoptosis, as indicated by a 10-fold increase in the percentage of cleaved caspase-3$^+$ cells (Fig. 1 B). The selective death of RGCs (Fig. 1 C) reflects a predominance of *Nf1* protein (neurofibromin) expression in RGCs within the retina (Fig. 1 D). Consistent with RGC death resulting from axonal injury, increased phospho-neurofilament heavy chain (pNF-H) immunostaining, a marker of axonal injury (Parrilla-Reverter et al., 2009), was observed in the optic nerves of female *Nf1*-OPG mice (Fig. 1 E).

Published December 6, 2016

In children with NF1, optical coherence tomography (OCT) is often used to monitor visual dysfunction secondary to OPG (Fisher et al., 2012). OCT measures the thickness of the RNFL (composed of RGC axons) and the inner plexiform layer/ganglion cell layer (IPL-GCL; Avery et al., 2011; Gu et al., 2014). Similar to the sexually dimorphic RGC effects, IPL-GCL and RNFL thicknesses were reduced by 34.2% (Fig. 1 F) and 52% (Fig. 1 G) in female *Nf1*-OPG mice, respectively, compared with controls. No significant differences were found between male *Nf1*-OPG mice and controls, as further demonstrated using retinal flat-mount preparations (SMI-32 immunostaining) and Western blotting (Fig. 1 H). Together, these observations establish that female *Nf1*-OPG mice exhibit greater tumor-induced axonal injury, leading to RGC loss and RNFL/IPL-GCL thinning.

Female gonadal sex hormones underlie the sexually dimorphic differences in *Nf1*-OPG–induced axonal damage and retinal dysfunction

Using the AOS strategy (Arnold, 2014), we first analyzed gonadal steroid hormones (estradiol, testosterone) as responsible etiologies. Although gonadal sex hormones are usually considered to function during or after puberty, there is an abundance of experimental data supporting critical roles for these hormones in brain neurons during fetal and early perinatal life in several vertebrate species (Bondesson et al., 2015). 4-vinylcyclohexene diepoxide (VCD) was initially used to chemically ablate ovarian function (Kappeler and Hoyer, 2012), which reduced RGC death (%TUNEL$^+$ cells) by 2.97-fold (Fig. 2 A) and increased RGC numbers (%Brn3a$^+$ cells) from 50 to 73% of WT levels (Fig. 1 A). Because VCD can have off-target effects, we performed surgical ovariectomies (OVX) of female *Nf1*-OPG mice, castration (Cast) of male *Nf1*-OPG mice, and respective sham surgeries at 6 wk of age. After male gonadectomy, serum testosterone levels decreased by 8.3-fold (Fig. 2 B); however, there was no change in RGC death (%TUNEL$^+$ cells and %Brn3a$^+$ cells) or RNFL thinning (Fig. 2 C). These results demonstrate that male gonadal sex hormones do not provide a neuroprotective effect for RGC survival in the setting of optic glioma. In contrast, OVX resulted in a 7.2-fold decrease in serum 17-β estradiol levels (Fig. 2 B) and a 4.3-fold reduction in the percentage of TUNEL$^+$ cells, increasing the percentage of Brn3a$^+$ cells from ∼50 to ∼77% and RNFL thickness from ∼46 to ∼100% of WT levels, respectively (Fig. 2 D).

Because girls and boys with NF1 are equally likely to develop an optic glioma (Diggs-Andrews et al., 2014b), we examined the optic gliomas in male and female *Nf1*-OPG mice. No differences were observed between male and female *Nf1*-OPG mice with respect to tumor penetrance, optic nerve volumes, proliferation, or astrocyte number (Fig. 2 E); however, OVX significantly affected glioma maintenance. Castrated males showed no differences in optic nerve volumes or proliferation (Fig. 2 F) or pNF-H immunostaining (Fig. 2 F), but OVX *Nf1*-OPG females exhibited a 42% decrease in optic nerve volume, a 70% decrease in proliferation, and reduced optic nerve pNF-H staining (Fig. 2 G). Collectively, these findings establish that gonadal sex hormones are critical for optic glioma growth, axonal damage, and retinal pathology in female *Nf1*-OPG mice.

Optic glioma–associated microglia activation underlie axonal damage and retinal dysfunction in *Nf1*-OPG mice

Microglia comprise 30–50% of the cells in human NF1-associated and sporadic low-grade gliomas (Simmons et al., 2011). Although their murine counterparts have slightly lower percentages of microglia (10–15% Iba1$^+$ cells), these *Nf1* mouse optic glioma–associated monocytes (Daginakatte and Gutmann, 2007) and their secreted chemokines (Ccl5; Solga et al., 2015) are critical for tumor maintenance. Based on these findings, we focused on microglia as potential cellular mediators of the observed sexually dimorphic effects.

First, we observed that female *Nf1*-OPG mice harbored 2.8-fold more optic glioma–associated microglia compared with their male counterparts (Fig. 3 A). Second, microglia numbers were also elevated in female, but not male, *Nf1*$^{+/-}$ optic nerves relative to their WT counterparts, even in the absence of an optic glioma (Fig. 3 B). Third, there was greater microglial activation (Daginakatte et al., 2008) in female *Nf1*-OPG mice, as indicated by a 3.2-fold increase in phospho-JNK$^+$ cells, relative to their male counterparts. However, Ccl5 expression did not differ between male and female *Nf1*-OPG mice, suggesting that this chemokine functions to support tumor growth in both males and females (unpublished data).

Because the proliferation and volumes of male and female murine optic gliomas were equivalent, we postulated that the relative increase in microglia and microglial activation might underlie the sexually dimorphic differences in optic glioma–induced retinal dysfunction. As such, previous studies have demonstrated that microglia can increase neuronal cell death and axonal injury in other experimental nervous system diseases (Neher et al., 2011; Schneider et al., 2015). Additionally, gonadal sex hormones, such as estrogen, have been previously implicated in brain microglia function (Tapia-Gonzalez et al., 2008; Saijo et al., 2011). To determine whether gonadectomy changes microglia content, we examined the percentage of Iba1$^+$ cells after gonadectomy. Although castration had no effect on microglial content, there was an approximately twofold decrease in the percentage of Iba1$^+$ cells after OVX, reducing microglia numbers to WT levels (Fig. 3 C). Additionally, the percentage of amoeboid-shaped (activated) microglia was reduced from 70 to 32% after OVX (Fig. 3 D).

To determine whether inhibition of microglia function could attenuate retinal dysfunction and axonal damage, female *Nf1*-OPG mice were treated with minocycline, a commonly used microglial pharmacologic inhibitor (Tikka et al., 2001). After treatment, there was a 1.7-fold decrease in the percentage of Iba1$^+$ cells (Fig. 3 E), decreased pNF-H immunostaining (Fig. 3 E), and a 3.9-fold decrease in the

Published December 6, 2016

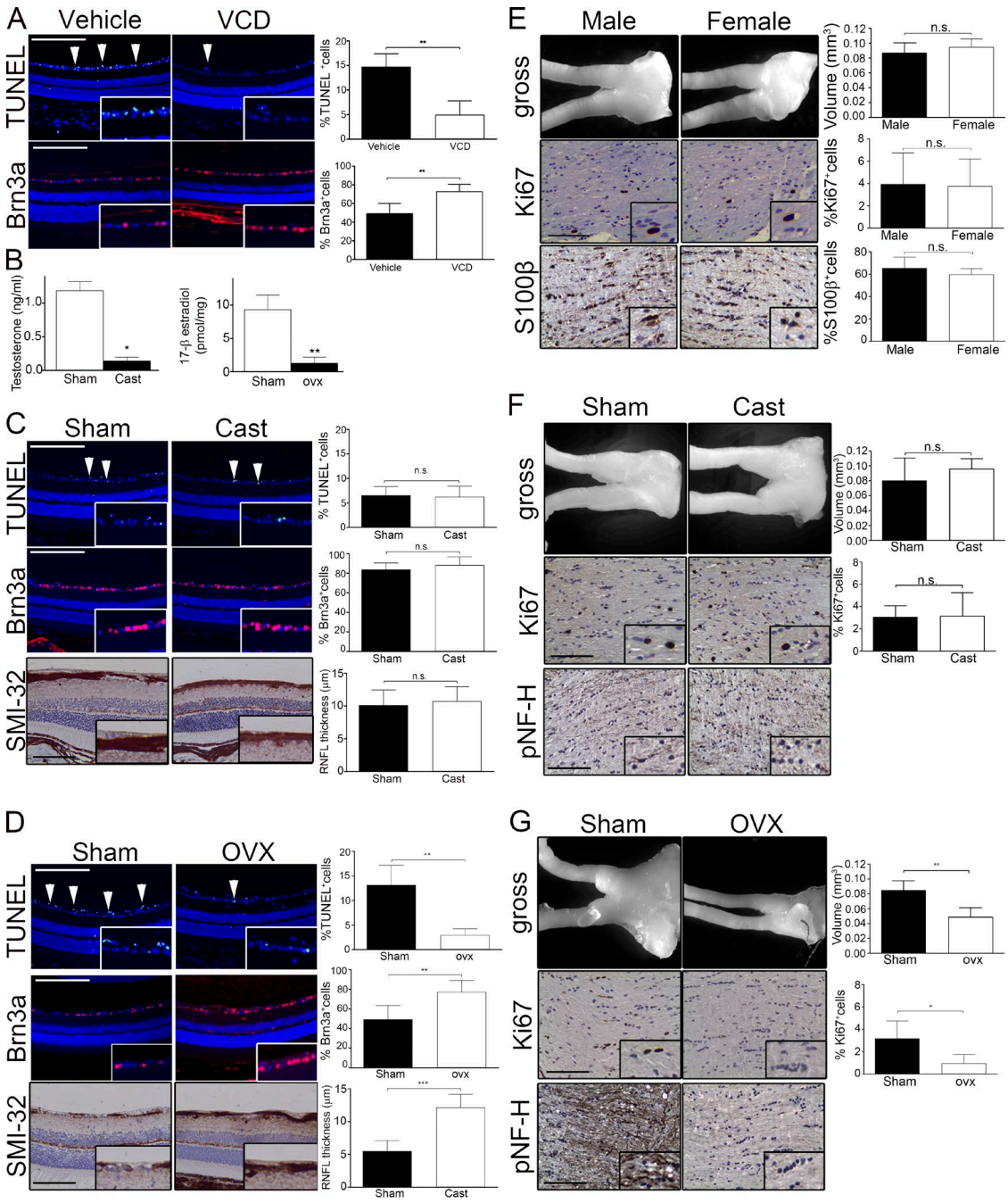

Figure 2. **Depletion of female gonadal sex hormones rescues tumor growth and RGC death in *Nf1*-OPG females.** (A) VCD treatment decreased TUNEL$^+$ cells in the RGC layer (Vehicle, 14.8 ± 2.7%; VCD, 4.9 ± 2.9; n = 6 mice) and increased the percentage of Brn3a$^+$ RGCs in FMC mice (Vehicle, 49.3 ± 10.8%; VCD, 73.1 ± 7.5; n = 7 mice/group). (B) Serum testosterone levels decreased after castration (Cast) of male *Nf1*-OPG mice (Sham, 1.19 ±0.14 ng/ml; Cast, 0.14 ± 0.05 ng/ml; n = 5 mice/group). Serum 17-β estradiol levels decreased after OVX of female *Nf1*-OPG mice (Sham, 9.33 ± 2.1 pmol/ml; OVX, 1.29 ± 0.88 pmol/ml; n = 7 mice/group). (C) Castration did not change retinal apoptosis (%TUNEL$^+$ cells; Sham, 6.53 ± 1.83; Cast, 6.25 ± 2.16; n = 7 mice), RGC loss (%Brn3a$^+$ cells; Sham, 83.78 ± 6.7; Cast, 86.21 ± 8.1; n = 7 mice/group), or RNFL thickness (SMI-32 staining; Sham, 10.14 ± 2.35 µm; Cast, 10.77 ± 2.2 µm; n = 7 mice/group). (D) OVX reduced RGC death (%TUNEL$^+$ cells; Sham, 13.19 ± 4.0; OVX, 2.98 ± 1.2; n = 7 mice/group), RGC loss (%Brn3a; Sham, 49.56 ± 13.9; OVX, 77.42 ± 11.7; n = 7 mice/group), and RNFL thinning (SMI-32 staining; Sham, 5.51 ± 1.6 µm; OVX, 12.2 ± 1.97 µm; n = 7 mice/group). (E) No differences in optic nerve volumes (Male, 0.087 ± 0.003 mm^3; Female, 0.095 ± 0.011 mm^3; n = 17 mice/group), %Ki67$^+$ cells (Male, 3.95 ± 2.81%; Female 3.76 ± 0.81%; n = 9 mice/group), or percentage of S100β$^+$ cells (Male, 65.35 ± 5.01%; Female, 59.81 ± 5.1%; n = 5 mice/group) were found in the optic nerves of male compared with female *Nf1*-OPG mice. (F) Optic nerve volume measurements (top; Sham, 0.084 ± 0.02 mm^3; Cast, 0.092 ± 0.02 mm^3; n = 6 mice/group), %Ki67$^+$ cells (middle; Sham, 3.08 ± 1.1%; Cast, 3.19 ± 2.08%; n = 6 mice/group), and pNF-H staining (bottom) within the optic nerve were

Published December 6, 2016

percentage of TUNEL$^+$ cells (Fig. 3 F). In addition, the percentage of Brn3a$^+$ cells increased from ∼40 to ∼70%, and RNFL thickness increased from ∼38 to ∼97% of WT levels, respectively (Fig. 3 F), thus establishing an essential role for microglia in mediating glioma maintenance (Daginakatte and Gutmann, 2007), as well as axonal damage, RGC death, and RNFL thinning, in response to murine optic glioma.

Estrogen acts through ERβ to activate optic nerve microglia in female *Nf1*-OPG mice

Estrogen can function either through its canonical (ERα and ERβ) receptors (Green et al., 1986; Kuiper et al., 1996) or via G-protein–coupled receptors (GPR30; Revankar et al., 2005). We first excluded GPR30 as a possible mediator using a selective GRP30 antagonist, G-15 (Dennis et al., 2009), and found that treatment of female *Nf1*-OPG mice did not change RGC apoptosis (unpublished data). Next, we focused on the ERα and ERβ receptors, which are both expressed in the optic nerve. However, ERβ is exclusively expressed in microglia (Wu et al., 2013), as confirmed herein using double-labeling immunohistochemistry (Fig. 4 A).

Two inflammatory cytokines (IL-1β and IL-6) implicated in neuronal apoptosis (Azevedo et al., 2013; Guadagno et al., 2015) are known to be regulated by ERβ engagement in brain microglia (Saijo et al., 2011). For this reason, we examined IL-1β (Fig. 4 B) and IL-6 (Fig. 4 C) levels, which were both elevated in the optic nerves of female, but not male, *Nf1*-OPG mice. To determine whether microglial activation, cytokine production, and subsequent neuronal damage were driven by ERβ activation, female *Nf1*-OPG mice were treated for 6 wk with 4-[2-phenyl-5,7-bis(trifluoromethyl) pyrazolo[1,5-a]-pyrimidin-3-yl]phenol (PHTPP), a selective ERβ antagonist (Compton et al., 2004). After treatment, there was a 2.4-fold decrease in the percentage of Iba1$^+$ cells, 20% decrease in optic nerve volumes, and 7.5-fold decrease in proliferation (%Ki67$^+$ cells), as well as reduced pNF-H staining and IL-1β/IL-6 expression (Fig. 4 D). The observed positive regulation of IL-1β in microglia by estradiol contrasts with other studies demonstrating negative regulation (Saijo et al., 2011; Zhao et al., 2016), which we postulate may reflect different disease contexts (experimental allergic encephalomyelitis versus neoplasia) and/or divergent mechanisms of estradiol signaling (GPR30 versus ERβ engagement).

Consistent with a critical role for microglia ERβ function in mediating neuronal cell death, ERβ inhibition decreased RGC apoptosis (%TUNEL$^+$ cells) to WT levels, increased the percentage of RGC number to 81% of WT levels, and increased the RNFL thickness from ∼44 to 100% of WT levels in *Nf1*-OPG mice (Fig. 4 E). Although it is not possible to completely separate the effects of ERβ activation on microglia-induced tumor growth from its effects on neuronal injury, these findings support a model in which microglia are critical drivers of glioma formation and maintenance in both male and female *Nf1* mice, likely through the actions of nonsexually dimorphic stromal factors (e.g., CCL5), whereas the tumor microenvironment created by ERβ-mediated release of neurotoxins (e.g., IL-1β and other inflammatory cytokines) facilitates the axonal injury, RGC death, RNFL thinning, and visual impairment observed in female *Nf1*-OPG mice.

In summary, these studies reveal critical roles for both estrogen and microglia in the neuronal injury response to optic glioma; however, the precise mechanism by which microglia create a neurotoxic environment, independent of tumor size, remains to be elucidated. Current studies are under way to examine specific inflammatory mediators (e.g., IL-1β and IL-6), as well as to define the transcriptional program of microglia in response to ERβ activation in the context of murine *Nf1*-OPG. The finding that female susceptibility to axonal injury, retinal pathology, and vision loss in the setting of optic glioma reflects estrogen activation of microglia represents one of the first demonstrations of sexually dimorphic differences in human disease. As the underlying molecular and cellular etiologies become clearer, potential neuroprotective strategies for reversing visual decline might emerge.

MATERIALS AND METHODS

Mice

Nf1$^{flox/mut}$;GFAP-Cre mice (*Nf1*$^{+/-}$ mice with somatic *Nf1* loss in neuroglial progenitor cells) were generated and maintained on a C57BL/6 background (Bajenaru et al., 2003). Analysis of mice was performed at 3 mo of age using independently generated cohorts. All animals were used in accordance with protocols approved by the animal studies committee at Washington University.

Pharmacological treatments

4-vinylcyclohexene diepoxide (VCD; 160 mg/kg; Sigma-Aldrich) diluted in corn oil (vehicle) was administered by i.p. injection for 20 consecutive d. Minocycline hydrochloride (50 mg/kg; Sigma-Aldrich) dissolved in sterile PBS was administered by i.p. injection for 5 d/week (2 wk), and controls received PBS injections. The selective ERβ antagonist PHTPP (4 mg/kg body weight; Sigma-Aldrich) was dissolved in corn oil and administered i.p. for 5 d/week (6 wk to 3 mo of age). Controls received i.p. corn oil injections.

unchanged after castration. (G) Optic nerve volumes (top; Sham, 0.085 ± 0.006 mm^3; OVX, 0.049 ± 0.004 mm^3; n = 5 mice/group) and %Ki67$^+$ cells (middle; Sham, 3.2 ± 0.64%; OVX, 0.96 ± 0.34%; n = 5 mice/group) were decreased after OVX. Axonal damage (pNF-H, bottom) was decreased after OVX of *Nf1*-OPG females relative to sham controls. Data in A–G were analyzed using a nonparametric Student's t test (Mann-Whitney). Similar results were obtained in a second independent experiment containing six mice per group. Bars, 100 µm. *, P < 0.05; **, P < 0.01; ***, P < 0.001; n.s., not significant.

Published December 6, 2016

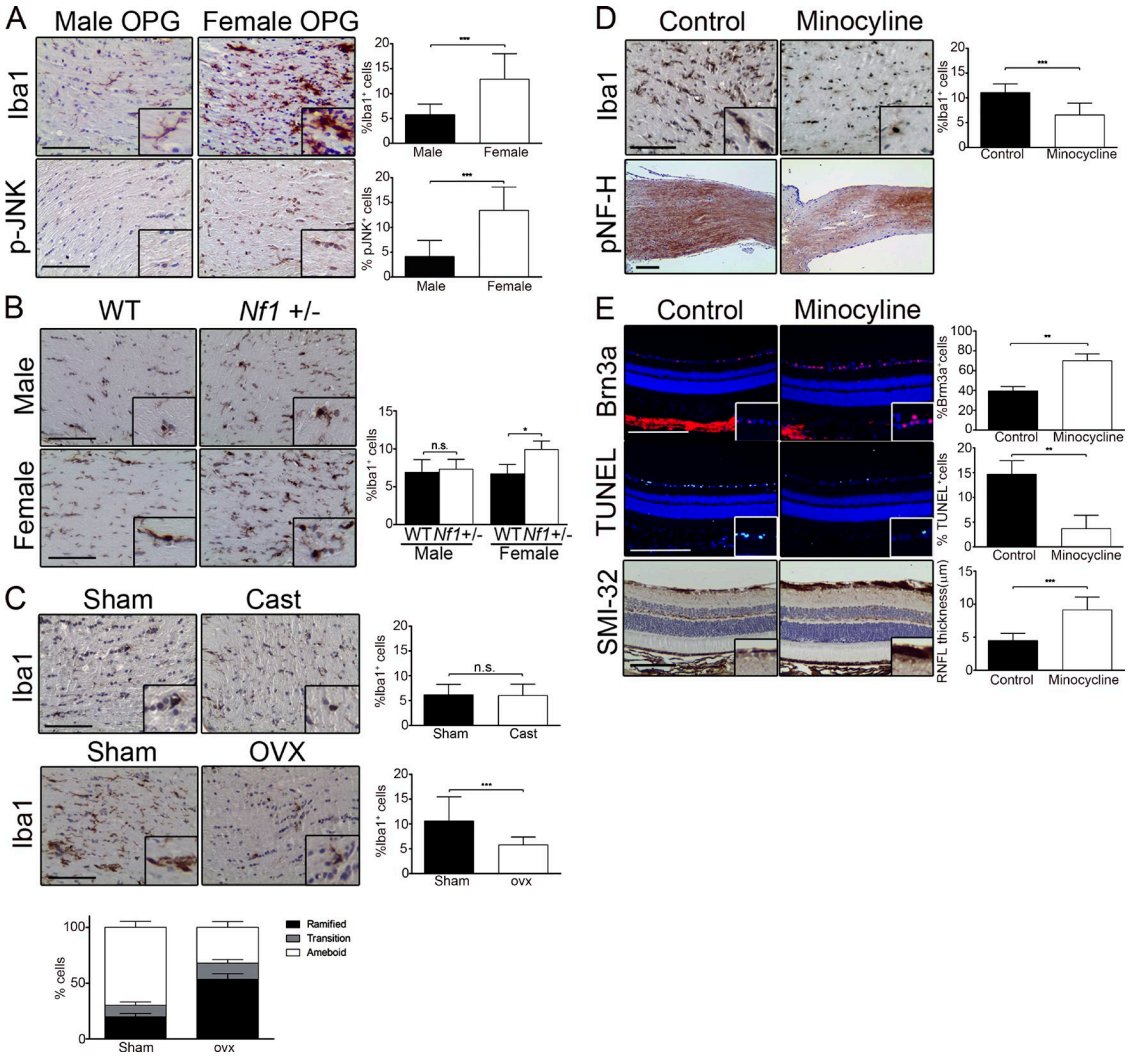

Figure 3. **Microglia causes axonal damage and RGC death in female *Nf1*-OPG mice.** (A) Optic nerves of female *Nf1*-OPG mice contained increased %Iba1$^+$ cells (Male, 5.8 ± 2.11%; Female, 12.96 ± 5.06%; n = 10 mice/group) and p-JNK$^+$ cells (Male, 4.16 ± 3.2%; Female, 13.5 ± 4.7%; n = 8 mice/group). (B) Immunostaining revealed increased Iba1$^+$ cells in *Nf1*$^{+/-}$ females compared with WT controls (WT, 6.7 ± 1.1%; *Nf1*$^{+/-}$, 9.9 ± 1.1%; n = 6 mice/group); however, no differences were observed in males (WT, 6.9 ± 1.7%; *Nf1*$^{+/-}$, 7.4 ± 1.3%). (C) The %Iba1$^+$ cells (top; Sham, 6.21 ± 2.05%; Cast, 6.1 ± 2.26%; n = 8 mice/group) did not differ between castrated *Nf1*-OPG males and sham controls. In contrast, the %Iba1$^+$ cells (bottom; Sham, 10.7 ± 4.84%; OVX, 5.83 ± 1.55%; n = 11 mice/group) were decreased after OVX in *Nf1*-OPG females compared with sham controls. Ramified microglia constitute 19.8% of the total microglia in sham *Nf1*-OPG female mice and 53.6% of the total microglia after OVX, whereas amoeboid or activated microglia are constituted 70% of the total microglia in sham *Nf1*-OPG optic nerves and 32% in OVX optic nerves (n = 6 mice/group). (D) Minocycline-treated female *Nf1*-OPG mice exhibited a decreased %Iba1$^+$ cells in the optic nerve (Control, 11.12 ± 1.71%; minocycline, 6.61 ± 2.3%; n = 8 mice/group) and axonal damage (pNF-H immunostaining). (E) After minocycline treatment, there was a reduction in the %TUNEL$^+$ cells (Control, 14.75 ± 1.1; minocycline, 3.75 ± 1.82; n = 6 mice/group), an increase in the %Brn3a$^+$ cells (Control, 39.79 ± 1.69%; minocycline, 70.42 ± 2.66%; n = 6 mice/group), and increased the RNFL thickness (SMI-32 staining; Control, 4.51 ± 1.1 µm; minocycline, 9.2 ± 1.9 µm; n = 8 mice/group). Data in A–E were analyzed using a nonparametric Student's t test (Mann-Whitney). Similar results were obtained in a second independent experiment containing five mice per group. Bars, 100 µm. *, P < 0.05; **, P < 0.01; ***, P < 0.001. n.s., not significant.

Western blotting

Retinae were microdissected and tissues were sonicated in 1% NP-40 buffer supplemented with protease and phosphatase inhibitors. Protein concentrations were determined using a BCA protein assay kit (Thermo Fisher Scientific), and Western blotting was performed as previously described using SMI-32 (BioLegend; 1:500 dilution; Daginakatte and Gutmann, 2007) antibodies and developed using chemiluminescence detection on a ChemiDoc-It Imaging System (UVP).

Retinal flat-mount staining

Eyes were fixed with 4% paraformaldehyde for 1 h and washed with PBS, and retinae were microdissected using 4 small incisions. Retinae were post-fixed in methanol and stored over-

Published December 6, 2016

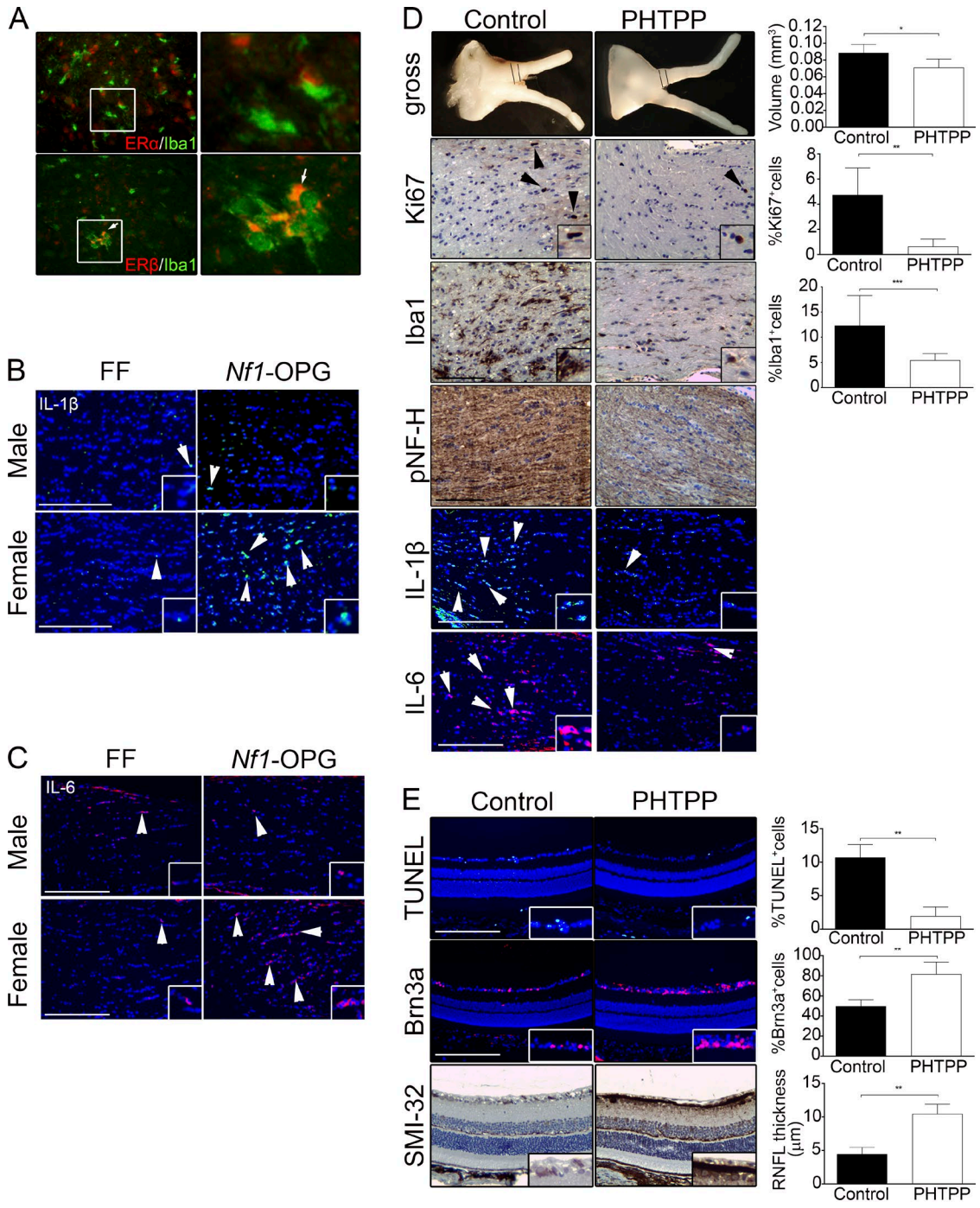

Figure 4. **Estrogen acts through ERβ to activate optic nerve microglia in female *Nf1*-OPG mice.** (A) Immunostaining for Iba1$^+$, ERα^+ double-labeled cells in the optic nerve (bottom, arrows). Immunostaining was performed for Il-1β (B) and Il-6 (C) in the optic nerves of FF male and female mice, as well as in *Nf1*-OPG male and female mice. (D) Optic nerves volumes (Control, 0.089 ± 0.02 mm^3; PHTPP, 0.071 ± 0.01 mm^3; n = 7 mice/group) and %Ki67$^+$ cells (Control, 4.75 ± 2.2%; PHTPP, 0.64 ± 0.59%; n = 6 mice/group) were decreased after PHTPP treatment (top). Microglia numbers (%Iba1$^+$ cells, Control, 12.33 ± 5.9; PHTPP, 5.44 ± 1.3, n = 8 mice/group), axonal injury (pNF-H), and IL-1β/IL-6 levels were decreased after treatment with PHTPP. (E) PHTPP treatment reduced the %TUNEL$^+$ cells (Control, 10.7 ± 0.78%; PHTPP, 1.95 ± 0.56%; n = 6 mice/group), increased the %Brn3a$^+$ cells (Control, 49.58 ± 2.69%; PHT PP, 81.7 ± 4.9%; n = 6 mice/group), and increased the RNFL thickness (SMI-32 staining; Control, 4.5 ± 0.4 µm; PHTPP, 10.5 ± 0.5 µm; n = 6 mice/group). Data in D and E were analyzed using a nonparametric Student's t test (Mann-Whitney). Similar results were obtained in a second independent experiment containing five mice per group. Bars, 100 µm. *, P < 0.05; **, P < 0.01; ***, P < 0.001. n.s., not significant.

night before incubation with SMI-32 antibody overnight (1:250) and immunofluorescent microscope imaging.

Castration and OVX

After anesthesia, 6-wk-old male mice were castrated by vas deferens cauterization using sterile surgical instruments in the Mouse Genetics Core at Washington University. Similarly, 6-wk-old female mice were surgically OVX and their fallopian tubes were ligated. Afterward, the skin was sutured and topical analgesics lidocaine ointment or bupivacaine were applied. Sham controls underwent identical procedures minus the gonadectomy.

Immunohistochemistry

After perfusion with Ringer's solution containing 0.1% lidocaine, 0.25% heparin, and 4% paraformaldehyde, optic nerves and eyeballs were post-fixed in 4% paraformaldehyde overnight. Tissues were embedded in paraffin and sectioned at 5 µm for immunostaining with the antibodies the following antibodies: Brn3a (1:500; Santa Cruz Biotechnology, Inc.), cleaved caspase-3 (1:250; R&D Biosystems), estrogen receptor α (1:200; Abcam), estrogen receptor β (1:200; Abcam), Iba1 (1:200; Novus Biologicals), Iba1 (1:1,000; Wako), IL-1β (1:200; Abcam), IL-6 (1:200; Santa Cruz Biotechnology, Inc.), Ki67 (1:500; BD), Neurofibromin (1:200; Santa Cruz Biotechnology, Inc.), pNF-H (1:1,000; Abcam), pSAPK-JNK (1:50; Cell Signaling Technology), SMI-32 (1:500; BioLegend). Biotinylated secondary antibodies (Vector Labs) were used for immunohistochemistry and developed using the Vectastain ABC kit. Alexa Fluor (Thermo Fisher Scientific) secondary antibodies were used for immunofluorescent staining. Terminal deoxynucleotide transferase–mediated dUTP nick ended (TUNEL) labeling (Roche) was performed as per the manufacturer's instructions.

Optic nerve measurements

Microdissected optic nerves were fixed in 4% paraformaldehyde overnight and then photographed, and diameters were measured beginning at the chiasm (and subsequently ∼150, ∼300, and ∼450 µm anterior to the chiasm) to generate optic nerve volumes as previously reported (Hegedus et al., 2008).

Retinal analyses

RNFL measurements were performed using ImageJ (National Institutes of Health) software on sections through the plain including pupil and optic nerves. Images were taken at 20× fields from 0 to 300 µm proximal to the optic nerve head. Repeated measurements of stained axons (SMI-32$^+$staining) were recorded and averaged for each area corresponding to each genotype.

Serum estradiol and testosterone assay

Serum was separated from whole blood after centrifugation and analyzed using 17β-Estradiol (Enzo Life Sciences) and Testosterone (Enzo Life Sciences) ELISA kits as per the manufacturer's protocol.

Statistical analysis

Statistical analysis was performed using Prism 5.0 software (GraphPad). Analyses involving only two groups were performed using nonparametric Student's *t* test (Mann–Whitney) and four groups were compared using a nonparametric one-way ANOVA (Kruskal–Wallis test) using Dunn's multiple comparison posttest. Statistical significance predetermined to be $P < 0.05$ for all statistical tests.

ACKNOWLEDGMENTS

This work was supported by Alex's Lemonade Stand Foundation and the National Cancer Institute (CA214146-01 and CA195692-01) to D.H. Gutmann. J.A. Toonen was supported by the Neurosciences T32 Training Grant (NS007205).

The authors declare no competing financial interests.

Submitted: 29 March 2016
Revised: 23 September 2016
Accepted: 11 November 2016

REFERENCES

Arnold, A.P. 2014. Conceptual frameworks and mouse models for studying sex differences in physiology and disease: why compensation changes the game. *Exp. Neurol.* 259:2–9. http://dx.doi.org/10.1016/j.expneurol.2014.01.021

Avery, R.A., G.T. Liu, M.J. Fisher, G.E. Quinn, J.B. Belasco, P.C. Phillips, M.G. Maguire, and L.J. Balcer. 2011. Retinal nerve fiber layer thickness in children with optic pathway gliomas. *Am. J. Ophthalmol.* 151:542–9.e2. http://dx.doi.org/10.1016/j.ajo.2010.08.046

Azevedo, E.P., J.H. Ledo, G. Barbosa, M. Sobrinho, L. Diniz, A.C. Fonseca, F. Gomes, L. Romão, F.R. Lima, F.L. Palhano, et al. 2013. Activated microglia mediate synapse loss and short-term memory deficits in a mouse model of transthyretin-related oculoleptomeningeal amyloidosis. *Cell Death Dis.* 4:e789. http://dx.doi.org/10.1038/cddis.2013.325

Bajenaru, M.L., M.R. Hernandez, A. Perry, Y. Zhu, L.F. Parada, J.R. Garbow, and D.H. Gutmann. 2003. Optic nerve glioma in mice requires astrocyte Nf1 gene inactivation and Nf1 brain heterozygosity. *Cancer Res.* 63:8573–8577.

Bondesson, M., R. Hao, C.Y. Lin, C. Williams, and J.A. Gustafsson. 2015. Estrogen receptor signaling during vertebrate development. *Biochim. Biophys. Acta.* 1849:142–151. http://dx.doi.org/10.1016/j.bbagrm.2014.06.005

Compton, D.R., S. Sheng, K.E. Carlson, N.A. Rebacz, I.Y. Lee, B.S. Katzenellenbogen, and J.A. Katzenellenbogen. 2004. Pyrazolo[1,5-a]pyrimidines: estrogen receptor ligands possessing estrogen receptor beta antagonist activity. *J. Med. Chem.* 47:5872–5893. http://dx.doi.org/10.1021/jm049631k

Daginakatte, G.C., and D.H. Gutmann. 2007. Neurofibromatosis-1 (Nf1) heterozygous brain microglia elaborate paracrine factors that promote Nf1-deficient astrocyte and glioma growth. *Hum. Mol. Genet.* 16:1098–1112. http://dx.doi.org/10.1093/hmg/ddm059

Daginakatte, G.C., S.M. Gianino, N.W. Zhao, A.S. Parsadanian, and D.H. Gutmann. 2008. Increased c-Jun-NH2-kinase signaling in neurofibromatosis-1 heterozygous microglia drives microglia activation and promotes optic glioma proliferation. *Cancer Res.* 68:10358–10366. http://dx.doi.org/10.1158/0008-5472.CAN-08-2506

Dennis, M.K., R. Burai, C. Ramesh, W.K. Petrie, S.N. Alcon, T.K. Nayak, C.G. Bologa, A. Leitao, E. Brailoiu, E. Deliu, et al. 2009. In vivo effects of a

GPR30 antagonist. *Nat. Chem. Biol.* 5:421–427. http://dx.doi.org/10.1038/nchembio.168

Diggs-Andrews, K.A., J.A. Brown, S.M. Gianino, L. D'Agostino McGowan, J.B. Rubin, D.F. Wozniak, and D.H. Gutmann. 2014a. Reply: To PMID 24375753. *Ann. Neurol.* 75:800–801. http://dx.doi.org/10.1002/ana.24156

Diggs-Andrews, K.A., J.A. Brown, S.M. Gianino, J.B. Rubin, D.F. Wozniak, and D.H. Gutmann. 2014b. Sex Is a major determinant of neuronal dysfunction in neurofibromatosis type 1. *Ann. Neurol.* 75:309–316. http://dx.doi.org/10.1002/ana.24093

Fisher, M.J., M. Loguidice, D.H. Gutmann, R. Listernick, R.E. Ferner, N.J. Ullrich, R.J. Packer, U. Tabori, R.O. Hoffman, S.L. Ardern-Holmes, et al. 2012. Visual outcomes in children with neurofibromatosis type 1-associated optic pathway glioma following chemotherapy: a multicenter retrospective analysis. *Neuro-oncol.* 14:790–797. http://dx.doi.org/10.1093/neuonc/nos076

Fisher, M.J., M. Loguidice, D.H. Gutmann, R. Listernick, R.E. Ferner, N.J. Ullrich, R.J. Packer, U. Tabori, R.O. Hoffman, S.L. Ardern-Holmes, et al. 2014. Gender as a disease modifier in neurofibromatosis type 1 optic pathway glioma. *Ann. Neurol.* 75:799–800. http://dx.doi.org/10.1002/ana.24157

Green, S., P. Walter, V. Kumar, A. Krust, J.M. Bornert, P. Argos, and P. Chambon. 1986. Human oestrogen receptor cDNA: sequence, expression and homology to v-erb-A. *Nature.* 320:134–139. http://dx.doi.org/10.1038/320134a0

Gu, S., N. Glaug, A. Cnaan, R.J. Packer, and R.A. Avery. 2014. Ganglion cell layer-inner plexiform layer thickness and vision loss in young children with optic pathway gliomas. *Invest. Ophthalmol. Vis. Sci.* 55:1402–1408. http://dx.doi.org/10.1167/iovs.13-13119

Guadagno, J., P. Swan, R. Shaikh, and S.P. Cregan. 2015. Microglia-derived IL-1β triggers p53-mediated cell cycle arrest and apoptosis in neural precursor cells. *Cell Death Dis.* 6:e1779. http://dx.doi.org/10.1038/cddis.2015.151

Hegedus, B., D. Banerjee, T.H. Yeh, S. Rothermich, A. Perry, J.B. Rubin, J.R. Garbow, and D.H. Gutmann. 2008. Preclinical cancer therapy in a mouse model of neurofibromatosis-1 optic glioma. *Cancer Res.* 68:1520–1528. http://dx.doi.org/10.1158/0008-5472.CAN-07-5916

Hyman, S.L., A. Shores, and K.N. North. 2005. The nature and frequency of cognitive deficits in children with neurofibromatosis type 1. *Neurology.* 65:1037–1044. http://dx.doi.org/10.1212/01.wnl.0000179303.72345.ce

Kalin-Hajdu, E., J.C. Décarie, M. Marzouki, A.S. Carret, and L.H. Ospina. 2014. Visual acuity of children treated with chemotherapy for optic pathway gliomas. *Pediatr. Blood Cancer.* 61:223–227. http://dx.doi.org/10.1002/pbc.24726

Kappeler, C.J., and P.B. Hoyer. 2012. 4-vinylcyclohexene diepoxide: a model chemical for ovotoxicity. *Syst Biol Reprod Med.* 58:57–62. http://dx.doi.org/10.3109/19396368.2011.648820

Kuiper, G.G., E. Enmark, M. Pelto-Huikko, S. Nilsson, and J.A. Gustafsson. 1996. Cloning of a novel receptor expressed in rat prostate and ovary. *Proc. Natl. Acad. Sci. USA.* 93:5925–5930. http://dx.doi.org/10.1073/pnas.93.12.5925

Listernick, R., J. Charrow, M. Greenwald, and M. Mets. 1994. Natural history of optic pathway tumors in children with neurofibromatosis type 1: a longitudinal study. *J. Pediatr.* 125:63–66. http://dx.doi.org/10.1016/S0022-3476(94)70122-9

Listernick, R., R.E. Ferner, G.T. Liu, and D.H. Gutmann. 2007. Optic pathway gliomas in neurofibromatosis-1: controversies and recommendations. *Ann. Neurol.* 61:189–198. http://dx.doi.org/10.1002/ana.21107

Neher, J.J., U. Neniskyte, J.W. Zhao, A. Bal-Price, A.M. Tolkovsky, and G.C. Brown. 2011. Inhibition of microglial phagocytosis is sufficient to prevent inflammatory neuronal death. *J. Immunol.* 186:4973–4983. http://dx.doi.org/10.4049/jimmunol.1003600

Parrilla-Reverter, G., M. Agudo, F. Nadal-Nicolás, L. Alarcón-Martínez, M. Jiménez-López, M. Salinas-Navarro, P. Sobrado-Calvo, J.M. Bernal-Garro, M.P. Villegas-Pérez, and M. Vidal-Sanz. 2009. Time-course of the retinal nerve fibre layer degeneration after complete intra-orbital optic nerve transection or crush: a comparative study. *Vision Res.* 49:2808–2825. http://dx.doi.org/10.1016/j.visres.2009.08.020

Revankar, C.M., D.F. Cimino, L.A. Sklar, J.B. Arterburn, and E.R. Prossnitz. 2005. A transmembrane intracellular estrogen receptor mediates rapid cell signaling. *Science.* 307:1625–1630. http://dx.doi.org/10.1126/science.1106943

Saijo, K., J.G. Collier, A.C. Li, J.A. Katzenellenbogen, and C.K. Glass. 2011. An ADIOL-ERβ-CtBP transrepression pathway negatively regulates microglia-mediated inflammation. *Cell.* 145:584–595. http://dx.doi.org/10.1016/j.cell.2011.03.050

Schneider, U.C., A.M. Davids, S. Brandenburg, A. Müller, A. Elke, S. Magrini, E. Atangana, K. Turkowski, T. Finger, A. Gutenberg, et al. 2015. Microglia inflict delayed brain injury after subarachnoid hemorrhage. *Acta Neuropathol.* 130:215–231. http://dx.doi.org/10.1007/s00401-015-1440-1

Simmons, G.W., W.W. Pong, R.J. Emnett, C.R. White, S.M. Gianino, F.J. Rodriguez, and D.H. Gutmann. 2011. Neurofibromatosis-1 heterozygosity increases microglia in a spatially and temporally restricted pattern relevant to mouse optic glioma formation and growth. *J. Neuropathol. Exp. Neurol.* 70:51–62. http://dx.doi.org/10.1097/NEN.0b013e3182032d37

Solga, A.C., W.W. Pong, K.Y. Kim, P.J. Cimino, J.A. Toonen, J. Walker, T. Wylie, V. Magrini, M. Griffith, O.L. Griffith, et al. 2015. RNA sequencing of tumor-associated microglia reveals Ccl5 as a stromal chemokine critical for neurofibromatosis-1 glioma growth. *Neoplasia.* 17:776–788. http://dx.doi.org/10.1016/j.neo.2015.10.002

Tapia-Gonzalez, S., P. Carrero, O. Pernia, L.M. Garcia-Segura, and Y. Diz-Chaves. 2008. Selective oestrogen receptor (ER) modulators reduce microglia reactivity in vivo after peripheral inflammation: potential role of microglial ERs. *J. Endocrinol.* 198:219–230. http://dx.doi.org/10.1677/JOE-07-0294

Tikka, T., B.L. Fiebich, G. Goldsteins, R. Keinanen, and J. Koistinaho. 2001. Minocycline, a tetracycline derivative, is neuroprotective against excitotoxicity by inhibiting activation and proliferation of microglia. *J. Neurosci.* 21:2580–2588.

Wu, W.F., X.J. Tan, Y.B. Dai, V. Krishnan, M. Warner, and J.A. Gustafsson. 2013. Targeting estrogen receptor β in microglia and T cells to treat experimental autoimmune encephalomyelitis. *Proc. Natl. Acad. Sci. USA.* 110:3543–3548. http://dx.doi.org/10.1073/pnas.1300313110

Zhao, T.Z., Q. Ding, J. Hu, S.M. He, F. Shi, and L.T. Ma. 2016. GPER expressed on microglia mediates the anti-inflammatory effect of estradiol in ischemic stroke. *Brain Behav.* 6:e00449. http://dx.doi.org/10.1002/brb3.449